

Molecular Cell, Volume 72

Supplemental Information

The BRCT Domains of the BRCA1 and BARD1 Tumor

Suppressors Differentially Regulate

Homology-Directed Repair and Stalled Fork Protection

David Billing, Michiko Horiguchi, Foon Wu-Baer, Angelo Tagliatela, Giuseppe Leuzzi, Silvia Alvarez Nanez, Wenxia Jiang, Shan Zha, Matthias Szabolcs, Chyuan-Sheng Lin, Alberto Ciccia, and Richard Baer

Figure S1, related to STAR Methods. The Brca1/Bard1 heterodimer.

A) A map of the mouse Brca1 and Bard1 proteins. The RING domains of Brca1 (amino acids 9-96) and Bard1 (36-110) are denoted as ovals, while the BRCT domains of Brca1 (1594-1786) and Bard1 (559-757) are shown as rectangles. The interaction between Brca1 and Bard1 is mediated by sequences encompassing their respective RING domains. The BRCT domain of Brca1 interacts in a mutually exclusive manner with the phosphorylated isoforms of several HDR proteins (Abraxas, Bach1, CtIP, Uhrf1) to form separate Brca1 complexes, while the BRCT domain of Bard1 interacts with poly(ADP-ribose) (PAR).

B) An alignment of the amino acid sequences encompassing the BRCT domains of Bard1 and Brca1 from both mouse (m) and human (h). The four conserved contact residues of the phosphate-binding cleft are highlighted in yellow, including amino acids S563, G564, T605, and K607 of mouse Bard1 and amino acids S1598, G1599, T1643, and K1645 of mouse Brca1. The three missense mutations examined in this study (Bard1-S563F, Bard1-K607A, and Brca1-S1598F) are highlighted in turquoise. The recognition sequence for HP1 binding in human BARD1 (PLVLI) is denoted in red.

C) The Bard1-S563F and Bard1-K607A mutations disrupt the interaction between mouse Bard1 and poly(ADP-ribose) chains (PAR). Purified glutathione S-transferase (GST) and GST-Bard1 fusion polypeptides containing the C-terminal region of murine Bard1 without (wt) or with (SF and KA) the indicated BRCT mutations were analyzed by PAGE (left). To assess their ability to interact with PAR (right), the indicated GST polypeptides were bound to glutathione-agarose beads and incubated with purified PAR chains. After elution from the beads with glutathione, the GST polypeptides were spotted onto a nitrocellulose membrane and immunoblotted with anti-PAR and, after stripping, anti-GST monoclonal antibody.

Figure S2, related to STAR Methods. Design of the mutant Bard1^{S563F} allele.

A) Map of the wild type *Bard1* locus (*Bard1*⁺) encompassing exons 7-9. The position of the wild type S563 codon in exon 8 is shown in green. The 5' and 3' *Bard1* DNA probes used for Southern analyses are shown, and relevant restriction enzyme sites are indicated: *EcoRV* (RV), *SacI*, *Scal*, *KpnI*, *PacI*, and *HindIII* (H3).

B) Map of the *Bard1*^{S563F-neo} targeting vector. The position of the S563F missense mutation in exon 8 is shown in red. A neomycin expression cassette flanked by *loxP* signals (purple triangles) was inserted into intron 7.

C) Map of the *Bard1*^{S563F-neo} allele generated by homologous recombination (HR).

D) Map of the *Bard1*^{S563F} allele generated by Cre-mediated recombination.

E) The sizes of the *EcoRV* fragments and *KpnI* fragments recognized, respectively, by the 5' and 3' *Bard1* DNA probes used for Southern analysis (shown in green in panels A-D).

Figure S3, related to STAR Methods. Design of the mutant Bard1^{K607A} allele.

A) Map of the wild type *Bard1* locus (*Bard1*⁺) encompassing exons 7-9. The position of the wild type K607 codon in exon 8 is shown in green. The 5' and 3' *Bard1* DNA probes used for Southern analyses are shown, and relevant restriction enzyme sites are indicated: *EcoRV* (RV), *SacI*, *Scal*, *KpnI*, *PacI*, and *HindIII* (H3).

B) Map of the *Bard1*^{K607A-neo} targeting vector. The position of the K607A missense mutation in exon 9 is shown in red. A neomycin expression cassette flanked by *loxP* signals (purple triangles) was inserted into intron 8.

C) Map of the *Bard1*^{K607A-neo} allele generated by homologous recombination (HR).

- D) Map of the *Bard1*^{K607A} allele generated by Cre-mediated recombination.
 E) The sizes of the *EcoRV* fragments and *KpnI* fragments recognized, respectively, by the 5' and 3' *Bard1* DNA probes used for Southern analysis (shown in green in panels A-D).

Figure S4, related to STAR Methods. *Bard1*^{SF/SF} and *Bard1*^{KA/KA} male mice display a fertility defect distinct from that of *Brca1*^{SF/SF} male mice.

A) The testes of six-week-old *Bard1*^{KA/KA}, *Bard1*^{SF/SF}, and *Brca1*^{SF/SF} mice are smaller than those of their wild type and heterozygous littermate controls.

B) H&E-stained transverse sections of seminiferous tubules from the testes of six-week-old mice at 20X magnification. Unlike those of wild type mice, all seminiferous tubules of *Brca1*^{SF/SF} mice were devoid of elongated spermatids and mature spermatozoa but contained all prior stages of germ cell development, including secondary spermatocytes and round spermatids. In contrast, the seminiferous tubules of *Bard1*^{SF/SF} and *Bard1*^{KA/KA} mice show two distinct patterns of maturation arrest. Approximately 50% of the tubules (arrows) were almost entirely devoid of germ cells, apart from a ring of spermatogonia adjacent to the basal membrane. The remaining tubules (asterisk) showed maturation arrest at the primary spermatocyte stage, with a complete absence of secondary spermatocytes, round spermatids, elongated spermatids, and spermatozoa. Scale bars = 100 micrometer.

C) Seminiferous tubules of *Bard1*^{+/+} (i), *Bard1*^{KA/KA} (ii, iii), *Brca1*^{SF/SF} (iv), and *Bard1*^{SF/SF} (v, vi) testes from 6-week-old mice shown at higher (40x) magnification. (i) *Bard1*^{+/+} tubules display normal germ cell maturation in all seminiferous tubules with production of elongated spermatids (arrowheads). Conversely, *Brca1*^{SF/SF} mice (iv) show germ cell maturation only up to the round spermatid stage (arrowheads) in all seminiferous tubules, some of which form multinucleated giant cells (arrow). Approximately half of the *Bard1*^{KA/KA} (ii) and *Bard1*^{SF/SF} (v) seminiferous tubules are largely acellular apart from a few spermatogonia (arrows) and Sertoli cells (arrowheads). The remaining *Bard1*^{KA/KA} (iii) and *Bard1*^{SF/SF} (vi) tubules exhibit a block in germ cell maturation at the pachytene stage of meiosis I in primary spermatocytes (arrow) with the characteristic coarse chromatin pattern representing the “thick threads” of chromosomal tetrads. Scale bars = 20 micrometer.

Figure S5, related to Figure 1. *Brca1* and *Bard1* expression and heterodimerization is preserved in *Bard1*^{SF/SF} and *Bard1*^{KA/KA} MEFs.

A) Subcellular fractionation of isogenic clones of *Bard1*^{+/+}, *Bard1*^{SF/+} and *Bard1*^{SF/SF} MEFs (left and middle) and *Bard1*^{+/+}, *Bard1*^{KA/+} and *Bard1*^{KA/KA} MEFs (right). Cytoplasmic and nuclear fractions were immunoblotted for *Brca1*, *Ctip*, *Bard1*, and tubulin. In all clones, *Brca1*, *Bard1*, and *Ctip* are properly localized in the nuclear fraction and absent from the cytoplasmic fraction.

B) Immunoprecipitation of whole cell lysates from isogenic clones of *Bard1*^{+/+}, *Bard1*^{SF/+} and *Bard1*^{SF/SF} MEFs (left panel) and *Bard1*^{+/+}, *Bard1*^{KA/+} and *Bard1*^{KA/KA} MEFs (right panel) with either the *Bard1*-specific antiserum (IP: *Bard1*) or the corresponding pre-immune serum (IP: pre). Immunoblotting was performed with either a *Brca1*- or *Ctip*-specific monoclonal antibody. The input represents 12.5% of the amount of cell lysate used for immunoprecipitation.

C) *Bard1*/*Mre11* co-immunoprecipitation analysis. *Bard1*^{+/+}, *Bard1*^{SF/SF}, and *Bard1*^{KA/KA} MEFs were irradiated with 10 Gy and harvested 1-hour post irradiation. Chromatin extracts were immunoprecipitated with either the *Bard1*-specific polyclonal rabbit antiserum (IP: *Bard1*) or the corresponding pre-immune serum (IP: pre), fractionated by PAGE, and immunoblotted with the

Mre11-specific monoclonal antibody. The inputs for the Bard1 and Mre11 immunoblots represent 0.33% and 1.2%, respectively, of the amount of chromatin extract used for immunoprecipitation. **D)** Bard1/HP1 γ co-immunoprecipitation analysis. Isogenic clones of *Bard1*^{+/+} and *Bard1*^{SF/SF} MEFs (left panels) and *Bard1*^{+/+} and *Bard1*^{KA/KA} MEFs (right panels) were irradiated with 10 Gy to induce the Bard1/HP1 γ interaction (Wu et al., 2015b) and harvested 1-hour post irradiation. Chromatin extracts were immunoprecipitated with either the HP1 γ -specific monoclonal antibody (IP: HP1 γ) or the non-specific M2 anti-Flag monoclonal antibody (IP: M2), fractionated by PAGE, and immunoblotted with either the Bard1-specific polyclonal antiserum or the HP1 γ -specific monoclonal antibody. The inputs for the Bard1 and HP1 γ immunoblots represent 6.3% and 16%, respectively, of the amount of chromatin extract used for immunoprecipitation.

Figure S6, related to Figure 1. Bard1^{KA/KA} cells are hypersensitive to DNA damaging agents and display genotoxin-induced chromosomal instability.

A) Colony survival analysis of MMC-treated isogenic *Bard1*^{+/+} and *Bard1*^{KA/KA} MEFs, along with isogenic *Brca1*^{+/+} and *Brca1*^{SF/SF} MEFs. Survival is quantified as the percentage of colonies on MMC-treated relative to untreated plates. Each experimental condition was plated in triplicate, and the error bars represent standard error of the mean.

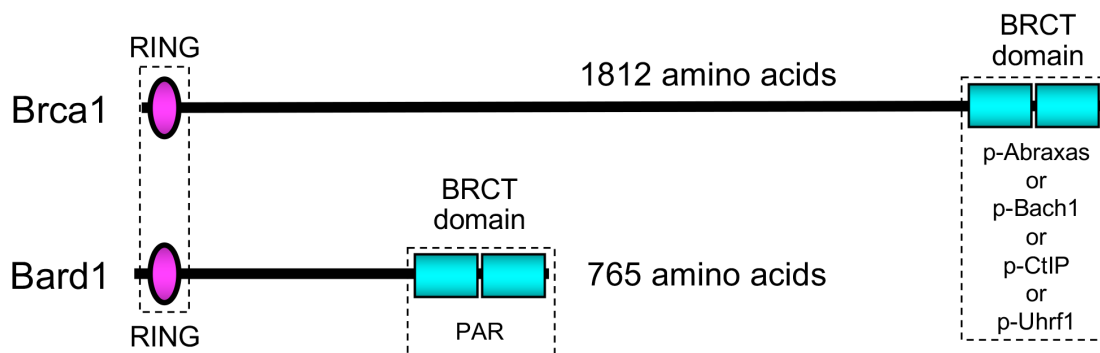
B) Colony survival analysis of olaparib-treated isogenic *Bard1*^{+/+} and *Bard1*^{KA/KA} MEFs, along with isogenic *Brca1*^{+/+} and *Brca1*^{SF/SF} MEFs.

C) Nuclear fractions of *Bard1*^{+/+}, *Bard1*^{Q552X/+}, and *Bard1*^{co-rec/+} MEFs were immunoblotted for Brca1, Bard1, PCNA, and histone H4.

D) Alkaline comet assay (as described in Figure 6) to assess HU-induced DNA damage in *Bard1*^{+/+}, *Bard1*^{Q552X/+}, *Bard1*^{co-rec/+}, *Bard1*^{SF/+}, and *Bard1*^{KA/+} MEFs. The mean tail moment is denoted by a horizontal red line and the standard error of the mean is indicated by error bars. Statistical analyses were conducted using one-way ANOVA (**** p<0.0001).

Figure S7, related to Figure 7. Model for tumorigenesis in a BRCA1 mutation carrier. All mammary epithelial cells (blue) of a *BRCA1* mutation carrier (*Brca1*^{mut/+}) are defective for SFP but competent for HDR. As a result of replication stress, *Brca1*^{mut/+} mammary epithelial cells experience some genome instability. In time, rare mutation(s) would arise that permit the viability of HDR-defective cells (such as loss of p53 or p16), allowing subsequent loss of the wild type *BRCA1* allele and the emergence of rare *Brca1*^{mut/-} variants (red) that are defective for both HDR and SFP. As such, these cells and their progeny would then experience more extensive genomic instability at levels sufficient to drive malignant progression.

A



B

556 **S563F** **K607A**

m-Bard1 **HP1** GPLVFIG**S**GLSSQOQKMLSKLETVLKAKKCMFEFSTVTHVIVP---DEEAQ**S**TLK**S**CMLGILSGCWILKFDWVKACLDISKVREQ
h-BARD1 **HP1** **PLVLI****S**GLSSEQOQKMLSELAVILKAKKYTEFSTVTHVVVP---GDAVQ**S**TLK**S**CMLGILNGCWILKFVWVKACLRKRVCEQ
h-BRCA1 KRMSMV**S**GLTPPEFMLVYKFARKHHITLNLITEETHVVMKTDAEFVCERTLKYFLGIAGGKWVVSYFVWTQSIKERKMLN
m-Brcal RDISMV**S**GLTPKEVMTVQKFAEKYRLTLTDAITEETHVIKTDAEFVCERTLKYFLGIAGGKWIVSYSWVVRSIQERRLLN

1591 **S1598F** 655

m-Bard1 EEKYEIVPG-----GPQRSRLNREQ-LLPKLFDGCFYFLGGNFKHHPRDDLKLI A AAGGKVL SRKPKPDS DVTQTINT
h-BARD1 EEKYEIPE-----GPRRSRLNREQ-LLPKLFDGCFYFLWGTFFKHHPKDNLIKLV TAGGGQILSRKPKPDS DVTQTINT
h-BRCA1 EHD FEVR-GDVVNGRNHQGPKRARE----SQRKIFRGL EICCYGPF TNPMTDQLEW MVQLCGASVVKELS-SFTLGTGV---
m-Brcal VHEFEVK-GDVVTGRNHQGP RR SRE----SREKLFKGLQVYCEPFTNP PKDELERMLQLCGASVVKELP-SLTHDTGA---

708 1698 765

m-Bard1 VAYHAKPESDQRFCTQYIVYEDL FNCHPERV RQ GK-----VWMAPSTWLI SCIMAFELLPLDS
h-BARD1 VAYHARPDSQRFCTQYIIYEDLCNYHPERV RQ GK-----VWKAPSSWFIDCVMSFELLPLDS
h-BRCA1 -----HPIVVVQPD AWTE DNGFHAIGOMCEAPVVTREWVLD SVALYQCQELD TYLIPQIPHSY
m-Brcal -----HLVVIVQPSAWTE DSNCPD IGQLCKARLVMWDWVLD SLSSYRCRDL DAYLVQNITCDSSEPQDSND

1747 1812

C

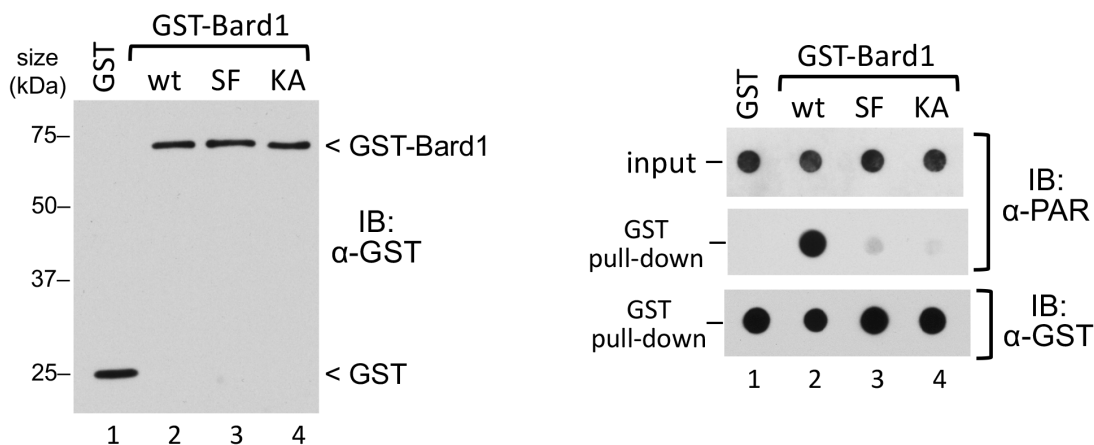


Figure S2

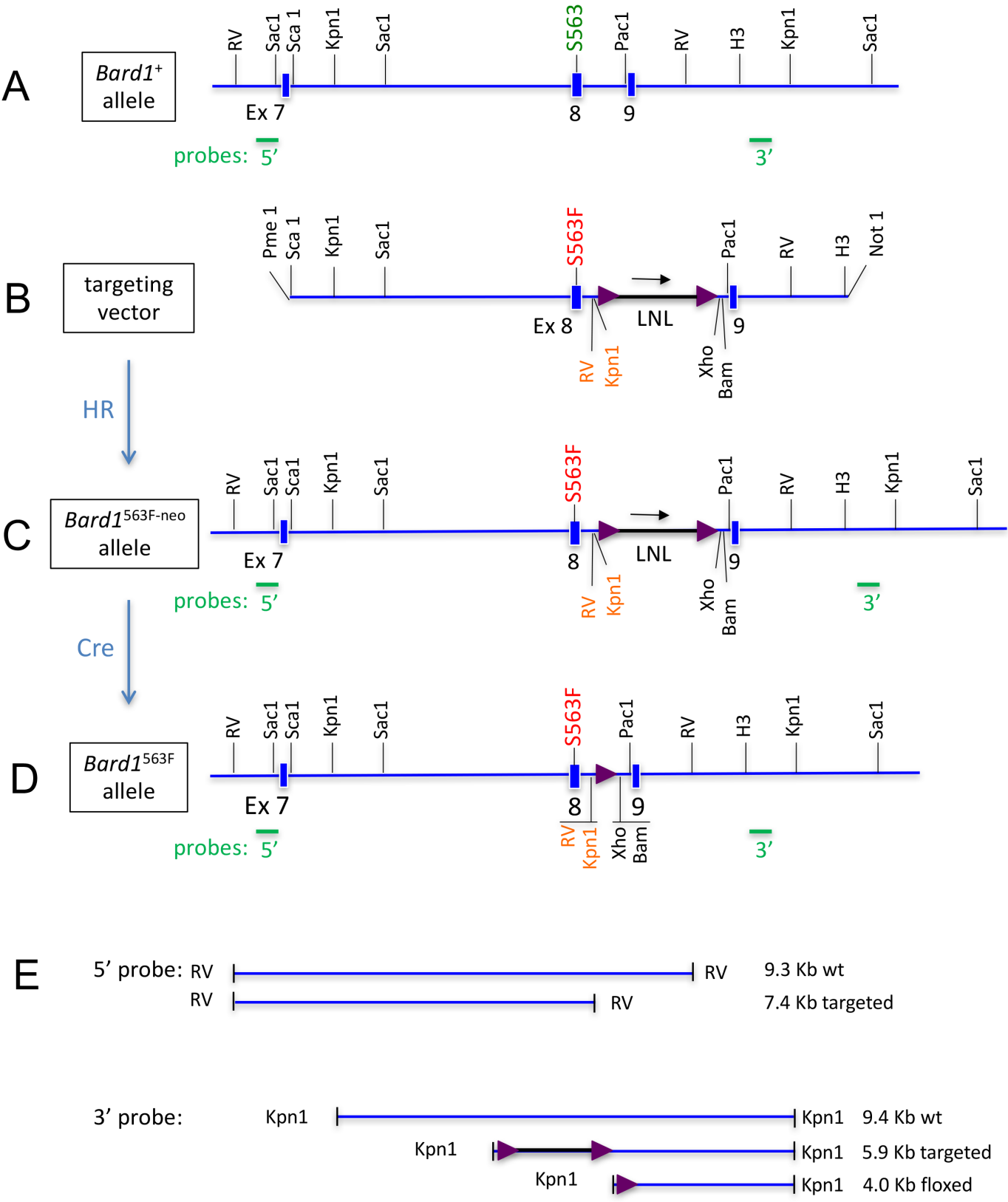


Figure S3

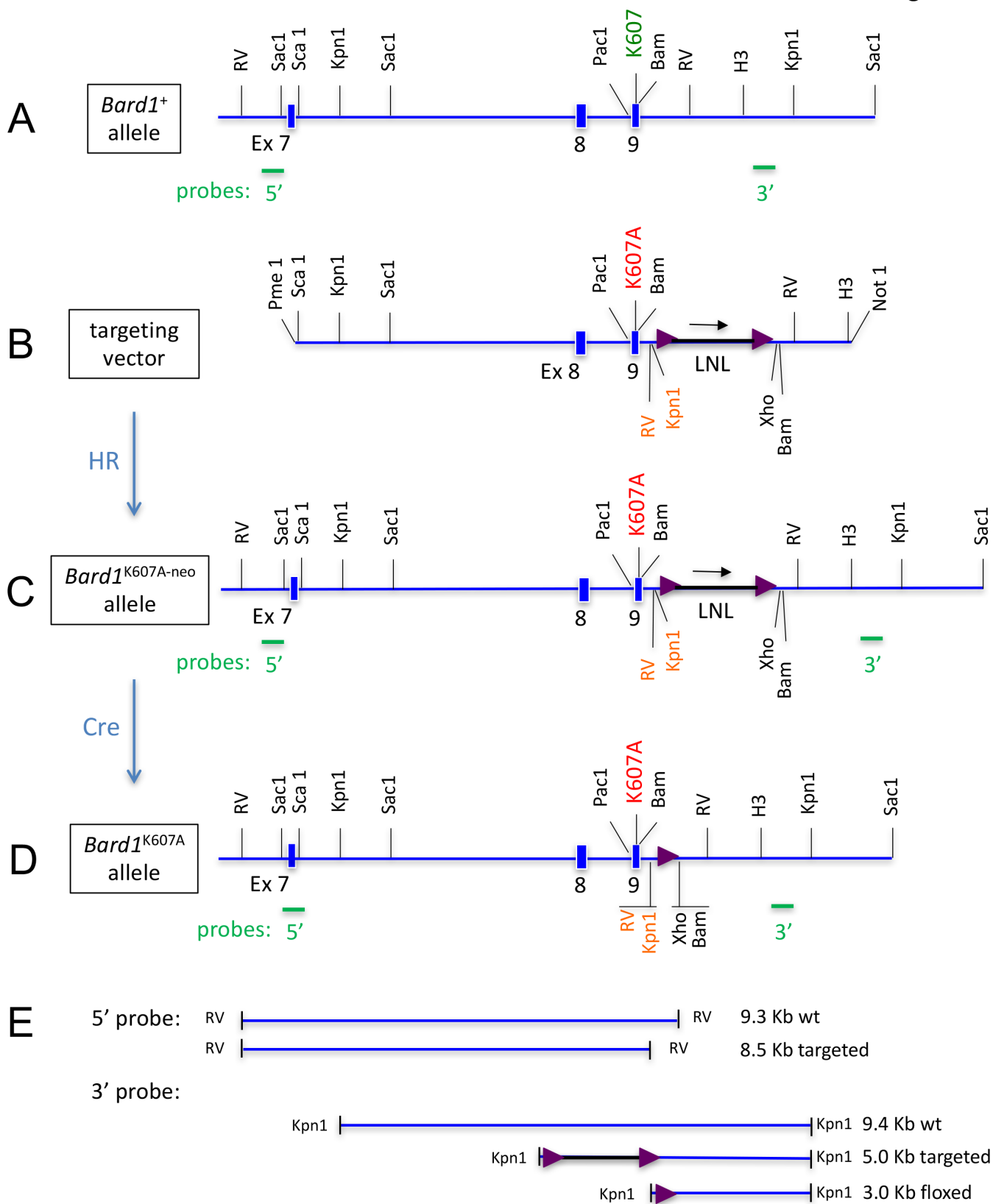


Figure S4

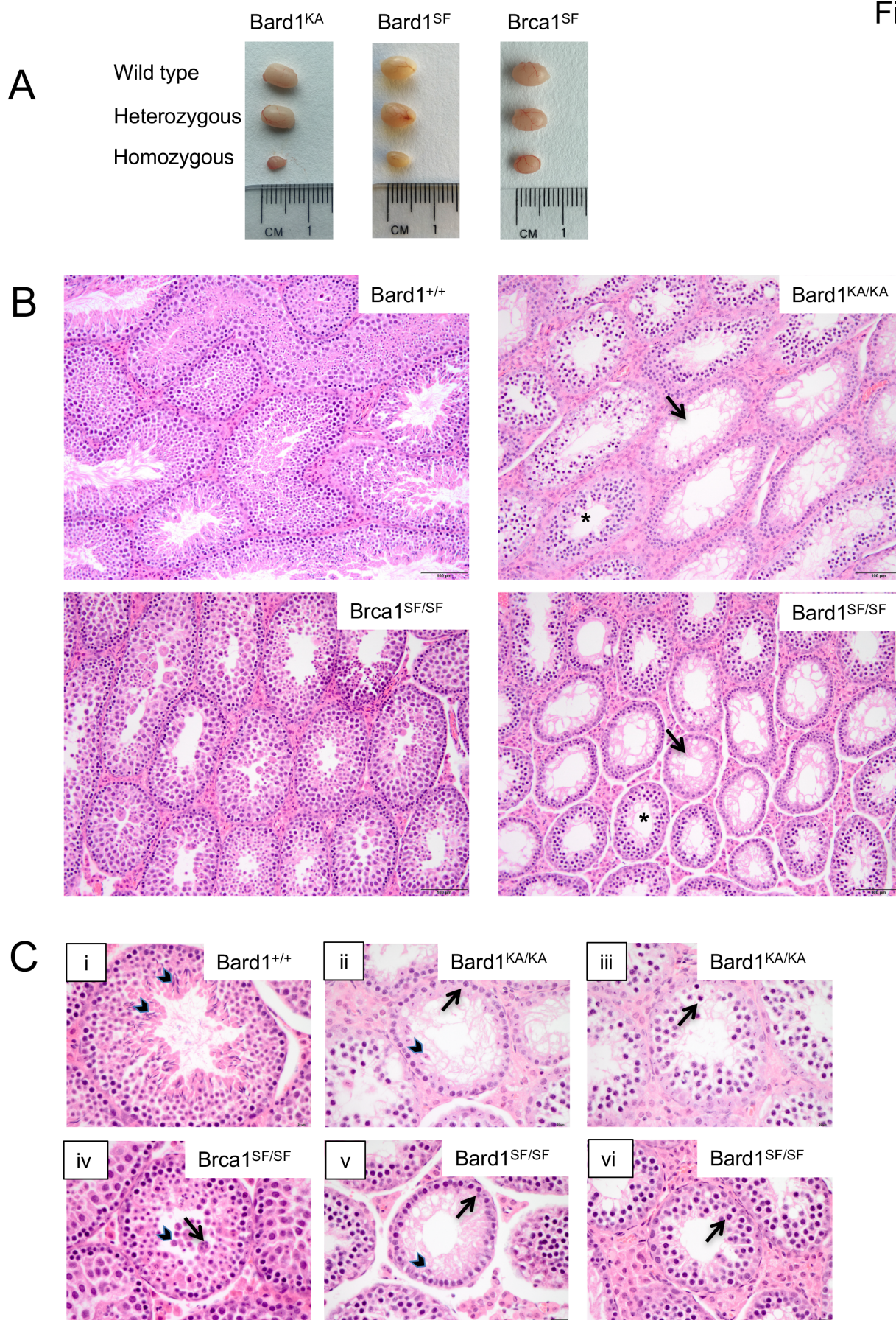


Figure S5

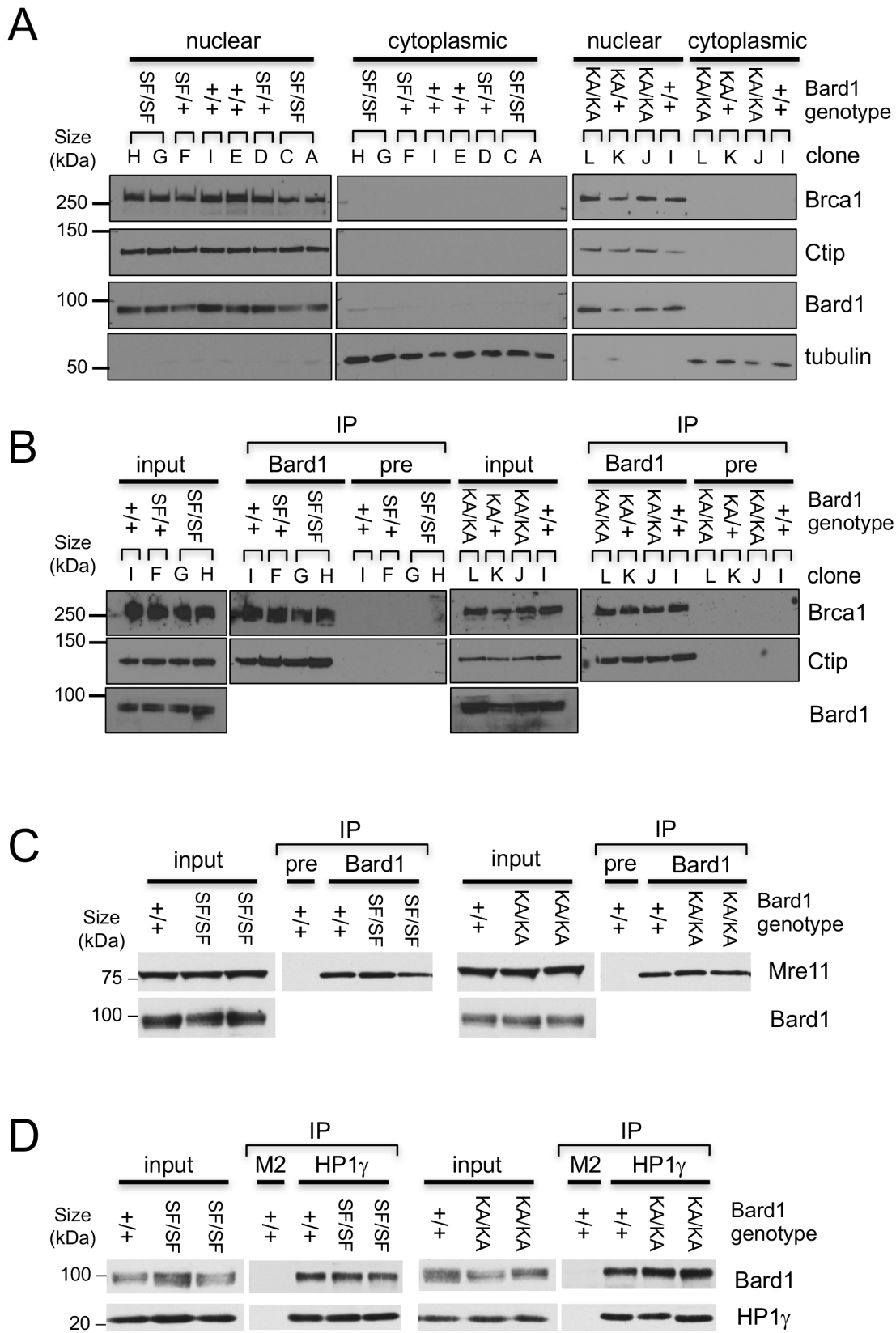
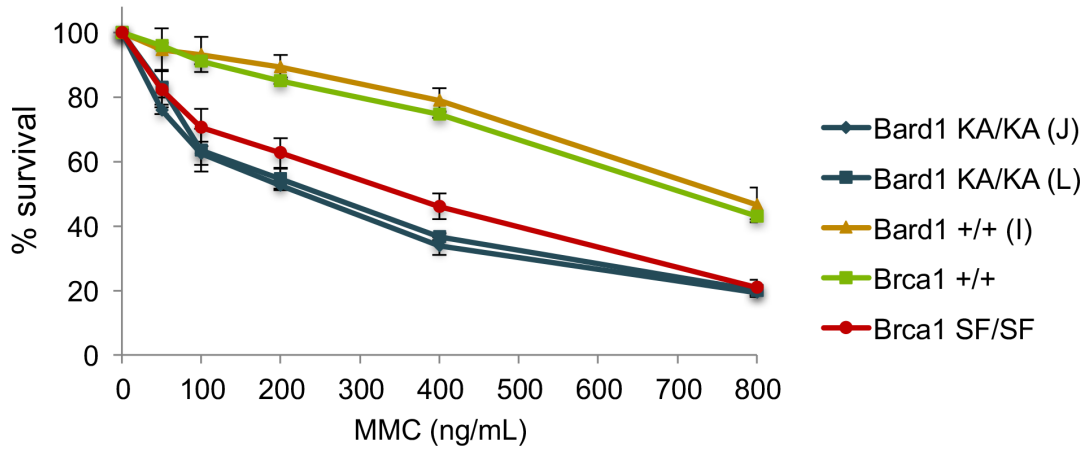
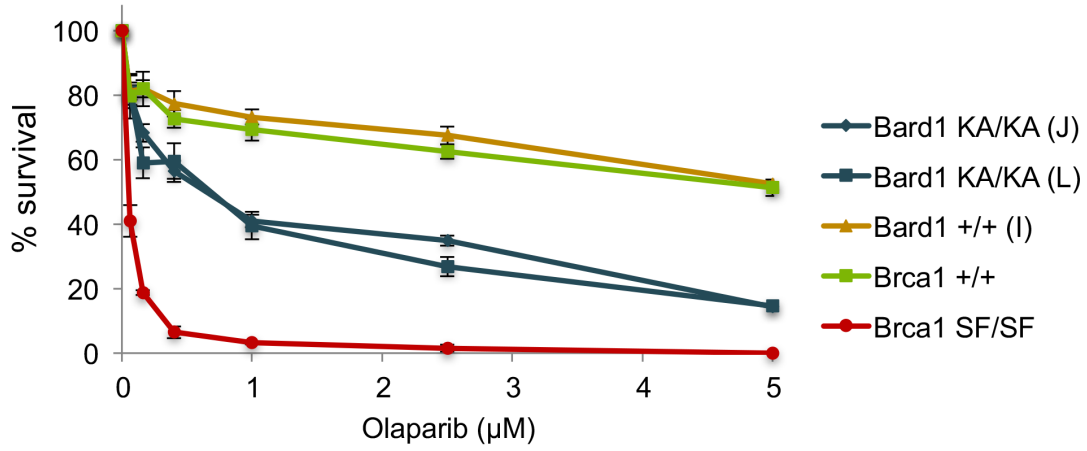


Figure S6

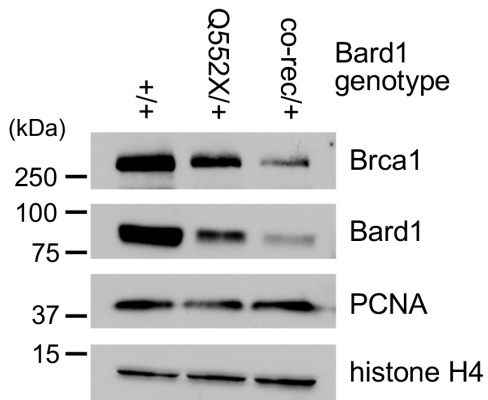
A



B



C



D

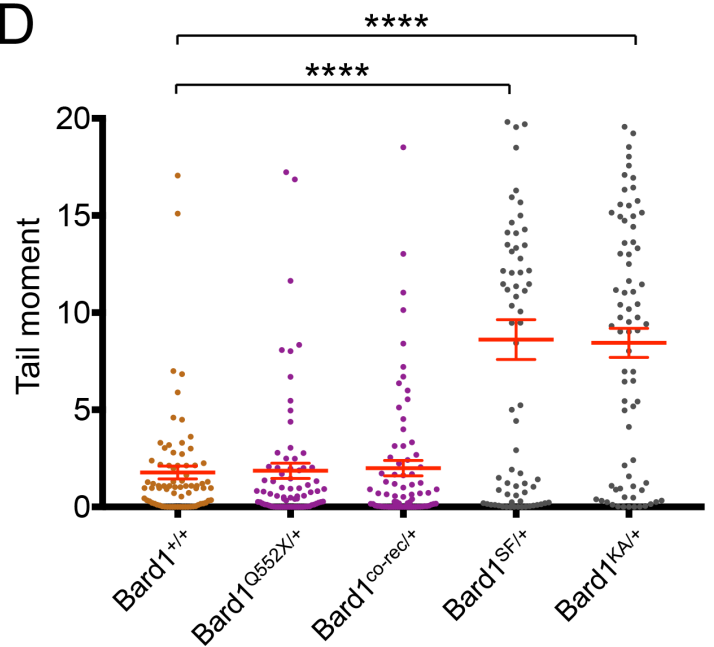


Figure S7

